



1 Evaluation of In-situ observations on Marine Weather Observer during 2 the Typhoon Sinlaku

3 Wenying He^{1,2}, Hongbin Chen^{1,2}, Hongyong Yu³, Jun Li¹, Jidong Pan¹, Shuqing Ma⁴,
4 Xuefen Zhang⁴, Rang Guo⁴, Bingke, Zhao⁵, Xi Chen⁶, Xiangao Xia^{1,2}, Kaicun Wang⁷
5 ¹Key Laboratory of Middle Atmosphere and Global Environment Observation, Institute of
6 Atmospheric Physic, Chinese Academy of Sciences, Beijing 100029, China
7 ²School of the Earth Science, Chinese Academy of Science University, Beijing 100049, China
8 ³State Key Laboratory of Earth Surface Processes and Resource Ecology, College of Global Change
9 and Earth System Science, Beijing Normal University, Beijing, China
10 ⁴Meteorological Observation Center of the China Meteorological Administration, Beijing 10081,
11 China
12 ⁵Shanghai Typhoon Institute of CMA, Shanghai 200030, China;
13 ⁶Shanghai Marine Meteorology Center, Shanghai Meteorology Center, Shanghai 200030, China;
14 ⁷Peking University, Beijing 100029, China

15
16 **Correspondence:** Wenying He (hwy@mail.iap.ac.cn) and Hongbin Chen (chb@mail.iap.ac.cn)
17

18 19 **Abstract**

20 The mobile ocean weather observation system, named Marine Weather Observer
21 (MWO), developed by the Institute of Atmospheric Physics (IAP), consists of a fully
22 solar-powered, unmanned vehicle and meteorological and hydrological instruments.
23 One of the MWOs completed a long-term continuous observation, actively
24 approaching the Typhoon Sinlaku center from July 24 to August 2, 2020, over the
25 South China Sea. The in-situ and high temporal resolution(1-min) observations
26 obtained from MWO were analyzed and evaluated by comparing with the observations
27 made by two types of buoys during the evolution of Typhoon Sinlaku. First, the air
28 pressure and wind speed measured by MWO are in good agreement with those
29 measured by the buoys before the typhoon, reflecting the equivalent measurement
30 capabilities of the two methods under normal sea conditions. The sea surface



31 temperature (SST) between MWO and the mooring buoys is highly consistent
32 throughout the observation period and even less difference after the typhoon's arrival,
33 indicating the high stability and accuracy of SST measurements from MWO during the
34 typhoon evolution. The air temperature and relative humidity measured by MWO have
35 significant diurnal variations, generally lower than those measured by the buoys,
36 which may be related to the mounting height of the sensor. When actively approaching
37 the typhoon center, the air pressure from MWO can reflect some drastic and subtle
38 changes, such as a sudden drop to 980 hPa, which is difficult to obtain by other
39 observation methods. As a mobile meteorological and oceanographic observation
40 station, MWO has shown its unique advantages over traditional observation methods,
41 and the results preliminary demonstrate the reliable observation capability of MWO in
42 this paper.

43

44 **1 Introduction**

45 Marine meteorological hazards, including typhoons, fog, strong winds, and many
46 other extreme weather events, occur frequently over China (Xu et al., 2009). In
47 particular, typhoons that make landfall off the southeast coast of China cause direct
48 economic losses of about 0.4% of gross domestic product and more than 500 deaths
49 per year (Lei, 2020). Many efforts have been made in recent decades to improve the
50 understanding of typhoon genesis and evolution and the forecasting of typhoon paths
51 (Bender et al. 2007; Black et al. 2007; Sanford et al. 2007; Bell et al. 2012). However,
52 errors in model initial conditions remain the main cause of typhoon forecast



53 uncertainty due to the scarcity of real-time ocean meteorological observations,
54 especially in distant waters (Zheng et al. 2008; Rogers et al. 2013; Emanuel and
55 Center 2018). Currently, marine observations over China are very limited and rarely
56 occur in the deep ocean (Dai et al., 2014). This situation greatly limits the
57 development of marine meteorology, especially the improvement of typhoon
58 forecasting. Therefore, there is a urgent need to develop advanced observation
59 techniques at sea. With the rapid development of satellite communication and
60 navigation technology as well as sensor technologies in recent years, marine
61 unmanned autonomous observation systems have been increasingly broken and
62 applied at sea (Lenan and Melville, 2014; Wynn et al., 2014; Thomson and Girton,
63 2017).

64 To obtain more meteorological observations at sea, the Institute of Atmospheric
65 Physics (IAP), Chinese Academy of Sciences, has developed an automatic and mobile
66 marine weather observations system based on a solar-powered, unmanned vehicle,
67 named Marine Weather Observer (MWO). To test the observation capability and
68 endurance, one of the MWOs cruised over the South China Sea from June to August
69 2020, during which a tropical cyclone formed and turned into a weak typhoon. The
70 MWO was then remotely controlled to actively approach the center of Typhoon
71 Sinlaku on August 1st, 2020, providing valuable in-situ observations for typhoon
72 research and forecasting (Chen et al., 2021, hereafter Chen21).

73 To better understand the quality of observations obtained from MWO, we directly
74 compared the observations of MWO and several buoys around it over the South China



75 Sea during the evolutions of Typhoon Sinlaku. The outline of the paper is described
76 below. In Section 2, we briefly describe Typhoon Sinlaku and the observations
77 obtained from MWO and the buoys. Then MWO observations and the comparisons
78 with buoys observations are presented in Section 3. The observation difference
79 between MWO and buoys are discussed in Section 4, and finally a summary is given
80 in Section 5.

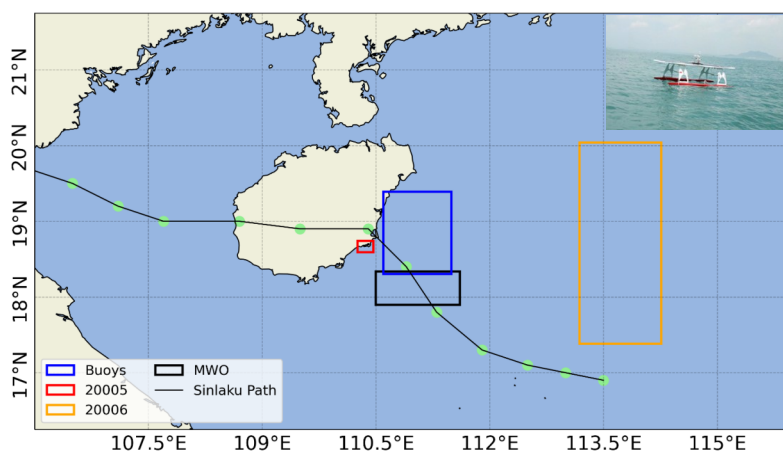
81 **2 Typhoon Sinlaku and the related observations**

82 Typhoon Sinlaku (No. 2003) formed as a tropical depression over the South
83 China Sea on July 31, 2020, then intensified into a typhoon on August 1. The center of
84 the typhoon crossed Hainan Island, China at a speed of 25 km/h and finally made
85 landfall off the coast of Thanh Hoa City, Vietnam, at 0840 UTC on August 2.

86 To better monitor the evolution of Typhoon Sinlaku, MWO was used for the first
87 time to obtain in-situ meteorological observations under extreme sea conditions. The
88 detailed MWO design and performance were described in Chen21. Measurements of
89 atmospheric and oceanic environment variables are accomplished with instruments
90 mounted on MWO, including the AirMar 220WX automatic weather station, mini-CT
91 sensor, and pyranometer. High temporal resolution (1 minute) data on atmospheric
92 temperature and humidity, air pressure, wind speed, wind direction, sea surface
93 temperature (SST), seawater conductivity, and total radiation can be automatically
94 transmitted to the ground control center via the Beidou communication satellite.
95 Detailed technical specifications of the meteorological and hydrological sensors can
96 be found in Chen21.



107 To evaluate the quality of the observations obtained from MWO, we mainly
108 compared them in this paper with the buoy observations conducted simultaneously
109 during the typhoon Sinlaku observation experiments from July 22 to August 4 (Zhang
110 et al., 2021, Qin et al., 2022). The buoy data consisted mainly of five mooring and two
111 drifting buoys that were able to provide the same environmental variables measured
112 on MWO from July 23 to August 2 but with a 10-minute interval. Thus, the 1-minute
113 observations from the MWO were averaged into 10-minute results and then matched
114 with the 10-minute observations from the buoys. More than 1300 matched samples at
10-minute intervals were obtained from July 24 to August 2, 2020, covering the main
evolution periods of Typhoon Sinlaku in the South China Sea.



107
108 Fig.1. Observation ranges of three observation methods, including 5 mooring buoys in the blue
109 box, 2 drifting buoys (20005 and 20006), and MWO(as shown in the small photo in the upper right
110 corner). The red, orange, and black boxes are the observation ranges of two drifting buoys and MWO
111 from July 24 to Aug.2, 2020, respectively. The light green dots on the black line are the locations of
112 Typhoon Sinlaku during the period from 0600UTC on July 31 to 0000 UTC on August 2, with a
113 3-hour interval.

114



115 From the locations and the observation ranges of the buoys and MWO in Fig.1, it
116 can be seen that for the two drifting buoys (20005 and 20006, named D05 and D06,
117 respectively), the drifting range of D05 is very close to the moving area of MWO,
118 while the drifting path of D06 is about 3-4 degree from MWO in longitude. For the
119 five mooring buoys in the blue box, one buoy named M64 is the closest, while the
120 others are located within about 100 km from MWO.

121

122 **3 Results**

123 **3.1 The observations from MWO**

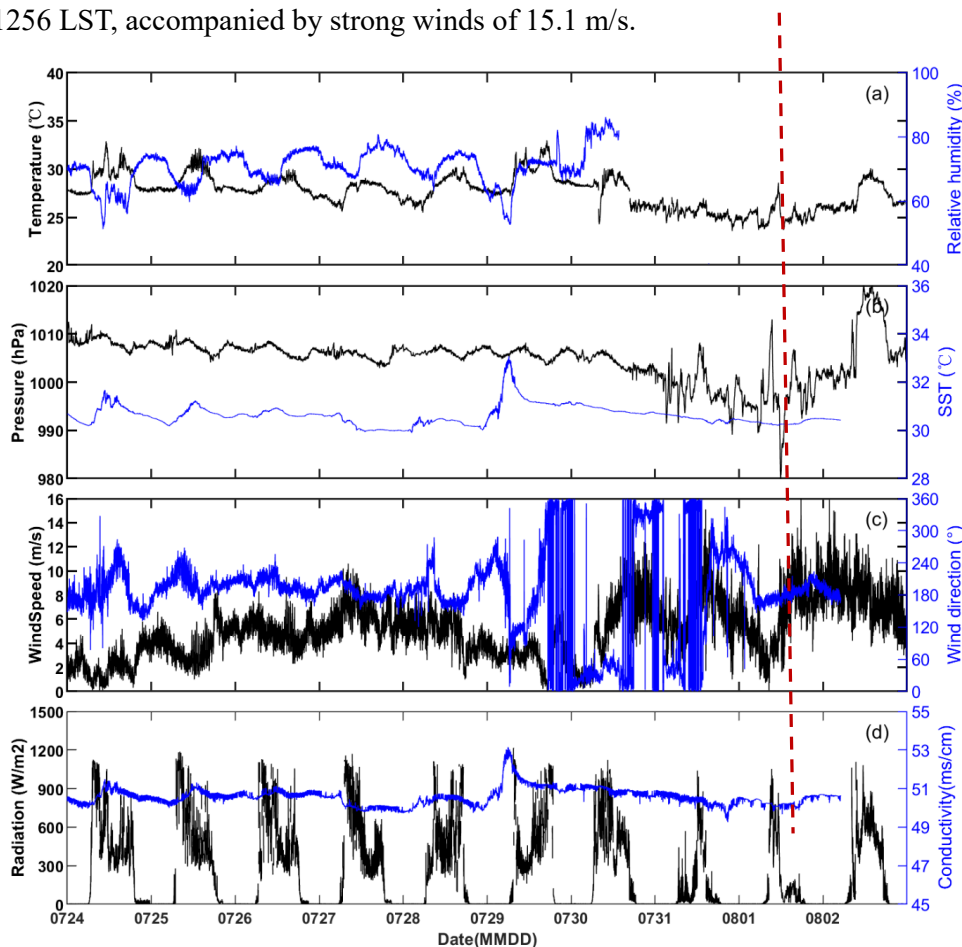
124 First, Fig.2 presents the time series of environmental variables measured by
125 MWO at **1-minute** interval from July 24 to August 2, 2020. It can be seen that in the
126 first stage before the arrival of the typhoon, such as July 24-29, the air temperature and
127 humidity show a clear diurnal variation and negative correlations, and the air pressure,
128 SST, and seawater conductivity also show small and stable variation.

129 Then from late July 29 to August 1, the typhoon moved toward the observation
130 area of MWO. The wind gradually strengthened, and the wind direction frequently
131 changed from south to north. The air pressure, air temperature, SST, and seawater
132 conductivity gradually decreased. On July 31, MWO was about 30 km away from
133 Typhoon Sinlaku and then actively moved to the predicted path of Sinlaku by remote
134 control. The drastic changes in air pressure and wind speed can be seen around noon
135 on August 1st. Unfortunately, the humidity sensor stopped working on July 31.

136 MWO arrived at the predicted passing area of Sinlaku on August 1st at 0928 LST



137 (Local Standard Time), with a pressure of 1011 hPa at that time. Then the air pressure
138 decreased to 992 hPa around 1140 LST and even rapidly dropped to the lowest 980
139 hPa at 1158 LST. Subsequently, the pressure gradually rose and increased to 992 hPa
140 at 1256 LST, accompanied by strong winds of 15.1 m/s.



141
142 **Fig.2.** Time series (LST) of (a) air temperature and relative humidity, (b) SST and atmospheric
143 pressure, (c) wind speed and direction, and (d) total radiation and seawater conductivity collected
144 onboard MWO in the **1-min interval** during the South China Sea typhoon observation experiment
145 from July 24 to August 02, 2020. The dashed red line represents the nearest times of MWO passing
146 through the typhoon center.

147
148 Such drastic fluctuations of air pressure over sea indicated that MWO might be
149 cross the typhoon center around 1200 LST. The subsequent path verification also



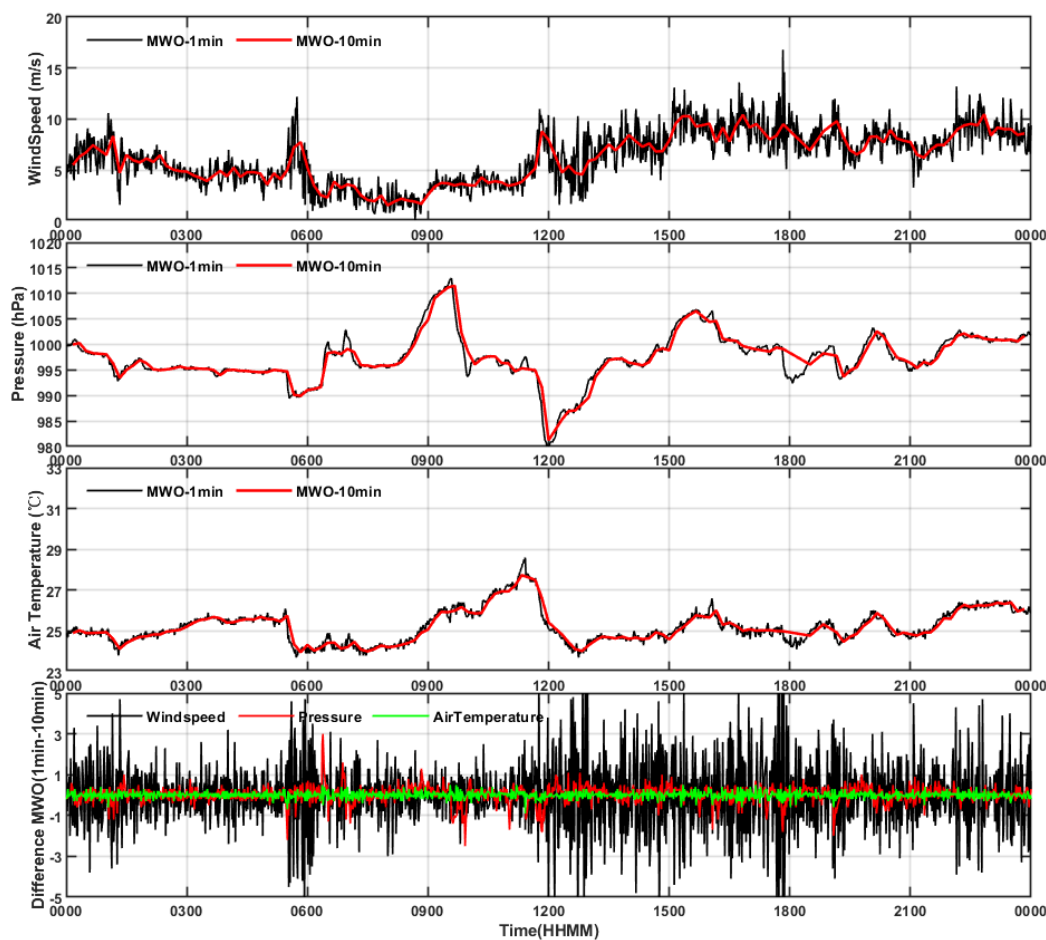
150 proved that MWO was nearly 2.4 km away from the typhoon path issued by the
151 Central Meteorological Observatory (CMO) of the China Meteorological
152 Administration, which reflected that MWO successfully passed through the center of
153 Typhoon Sinlaku. When Sinlaku was moved away from MWO observation range on
154 August 2, the wind speed gradually decreased and varied less in direction. Compared
155 with the normal sea conditions in the first stage, we call the next four days (from July
156 30 to Aug.2) as the second stage with larger changes in sea conditions.

157 To match the 10-minute observations from the buoy, we reprocessed the 1-minute
158 observations provided by MWO to the 10-minute average. Usually, under stable sea
159 conditions, the differences in meteorological variables over time may be slight in the
160 short term. When the typhoon arrived on August 1 and MWO approached the typhoon
161 center, the variables measured on MWO showed significant changes in Fig. 2.
162 Therefore, the difference between 1-minute and 10-minute averaged meteorological
163 variables may be useful for detecting fine-scale structure during typhoons.

164 Thus, the differences between the 1-minute and 10-minute results for the three
165 variables, including wind speed, air pressure, and air temperature on August 1 are
166 shown in Fig.3. It is clear that the trends in air pressure (Fig.3b) are consistent for both
167 time windows, for example, there are two peaks from 0600 LST to 1000 LST and a
168 sharp drop to 980 hPa around 1200 LST. the air temperature in Fig.3c also shows a
169 highly consistent variation in the 1-min and 10-min results. However, there is a
170 significant difference in the wind speed between the two time windows (Fig. 3a).
171 Before 1200 LST, both wind speeds are close to each other and are relatively



172 consistent. As the MWO approaches the typhoon center after 1200 LST, the 1-minute
173 wind speed varies more significantly than the 10-minute wind speed until 1800 LST. It
174 is assumed that the 10-minute window may reflect the average state of the wind field
175 to some extent. The significant difference between the 1-minute and 10-minute wind
176 speeds reflects the changes in the fine-scale structure of the wind field during the
177 typhoon evolution. As shown in Fig. 3d, the differences in pressure and temperature in
178 the two time windows were mostly close to zero and did not vary much throughout the
179 day on August 1. In contrast, the wind speed varies greatly with different time interval
180 during most of the day, especially around 0600 LST and 1200-1800 LST, where the
181 wind speed difference is as high as 5 m/s. This also reflects the apparent fluctuating
182 behavior of the 1-minute wind field, indicating strong turbulent activity in the
183 near-surface atmosphere. There has been a lot of research work on horizontal roll and
184 tornado-scale vortices of typhoons, which are closely related to the drastic changes in
185 the wind field (Morrison et al. 2005; Lorsolo et al. 2008; Wurman and Kosiba 2018;
186 Wu et al. 2020). Most of the previous work has been based mainly on landfalling
187 hurricanes observed by Doppler radar deployed near the coast. In this work, in situ
188 observations of MWOs that can actively cross typhoon centers in distant oceanic
189 regions will provide a new perspective to study the fine structural changes during
190 typhoon evolution.



191

192 Fig.3 The difference between 1-min and 10-min results for wind speed, air pressure, and temperature
193 on Aug.1.

194

195 3.2 Comparisons of the observations between MWO and buoys

196 To assess the quality of MWO observations, we first compared the air pressure
197 and wind speed measured by MWO and all buoys (drifting and moored) as shown in
198 Fig. 4. Before seeing the differences in the observations, it is best to know the spatial
199 distance variation between MWO and the buoys as shown in Fig. 4c. For the two
200 drifting buoys, the D05 was always closer to the MWO, within 100 km, from July 24



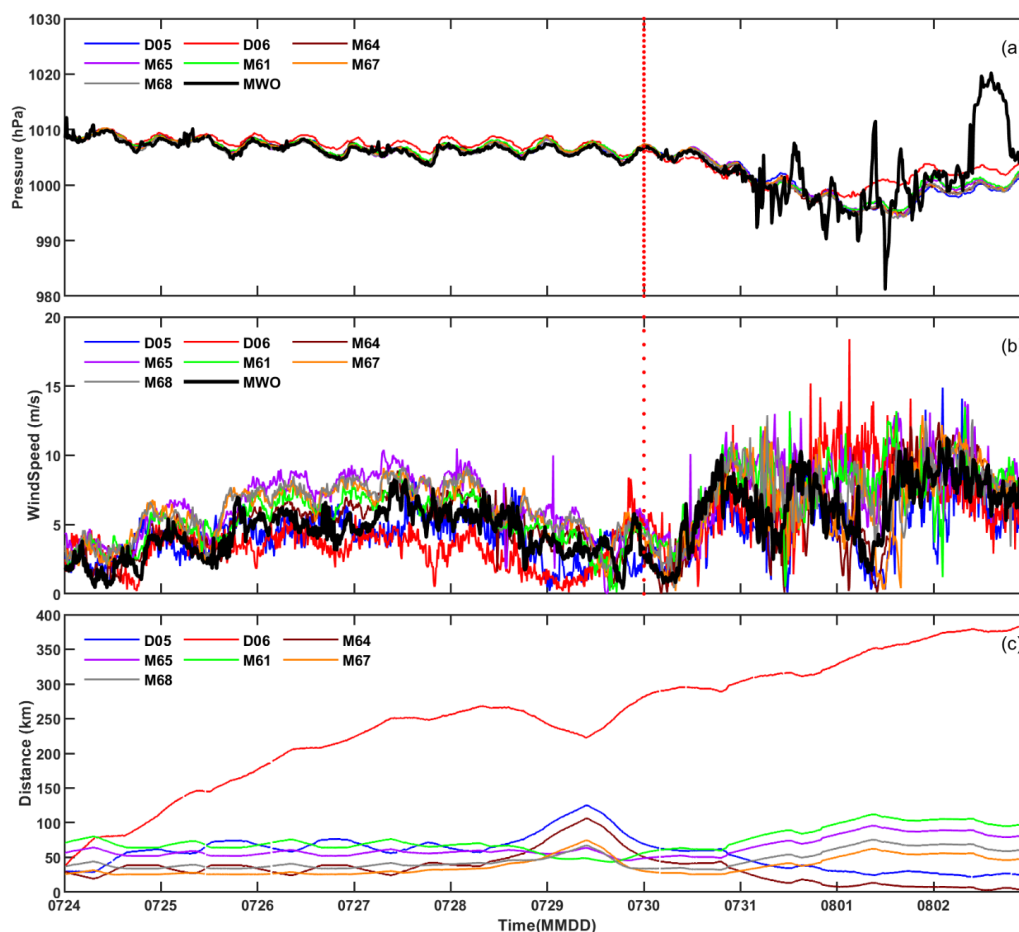
201 to August 2. While D06 gradually moved away from MWO over time, from less than
202 100 km on July 24 to 400 km on August 2. For the five mooring buoys, M64 is less
203 than 50 km from MWO from July 24 to 31 and very close to MWO from August 1 to 2.
204 The rest of the buoys are within 100 km from MWO.

205 Then for the air pressure comparison in Fig. 4a, all buoys and the MWO
206 measurements in the first stage match very well and basically overlap, except for a
207 slight difference in the farthest D06. With the arrival of the typhoon, the measured
208 pressure from MWO changed more obviously, especially around 1200 LST on August
209 1 the lowest pressure was about 980 hPa when MWO was close to the typhoon center.
210 In addition, an abnormally high pressure was measured on MWO around 14:00 on
211 August 2, and the cause of the abnormality is unknown at present. The pressure
212 measured by the buoys was relatively close and consistent throughout the period,
213 except for a slight change in the farthest buoy D06.

214 The wind speeds measured from buoys and MWO (Fig.4b) have a good
215 consistency. They are very close to each other in the first stage due to stable sea
216 conditions, especially the closer buoys D05 and M64. In the second stage, especially
217 from July 31 to August 1, there are enhanced changes in wind speed due to the passing
218 of the typhoon. In the first half of August 1st, there was a significant trend difference
219 in wind speed from MWO and buoys, for example, the former gradually decreased and
220 reached its minimum value when MWO is closing to the typhoon center about 1200
221 LST, while the latter mostly increased during this period. Subsequently, in the second
222 half of August 1st, the wind speed from MWO rapidly increases to 10m/s, more



223 consistent with those measured from buoys and almost superimposed. As the typhoon
224 gradually moved away from the observation domain of MWO and buoys on Aug.2, all
225 wind speeds became closer and gradually decreased, returning to the first stage state.



226
227 **Fig.4.** Time series (LST) of (a) air pressure and (b) wind speed collected from seven buoys (2
228 drifting and 5 mooring, legend begin with D and M, respectively) and MWO from July 24 to August
229 02, 2020. The dashed red line is on July 30 to separate the first and second stages.
230

231 Similarly, air temperature and SST obtained from MWO and buoys are compared
232 in Fig.5. It seems in Fig.5a that air temperature from MWO is generally lower than
233 those from buoys most of the time, especially during the night of the first stage and



234 when approaching the center of the typhoon in the second stage. The diurnal variations
235 of air temperature measured from MWO and the drifting buoy D05 are more
236 significant and close in the first stage. Relatively, the air temperature differences
237 among the mooring buoys are smaller and more stable in the first stage, then enhanced
238 due to the coming of the typhoon.

239 For SST shown in Fig.5b, the observations from MWO during the entire period
240 are very close to those from the five mooring buoys, and are more consistent, even
241 showing peak areas simultaneously, except for the slight difference from July 27-29.
242 For the two drifting buoys, the SST measured by the D05 buoy is 1-2 °C lower than
243 that measured by MWO on July 27-30, while SST measured by the D06 buoy is more
244 stable and close to that measured by MWO.

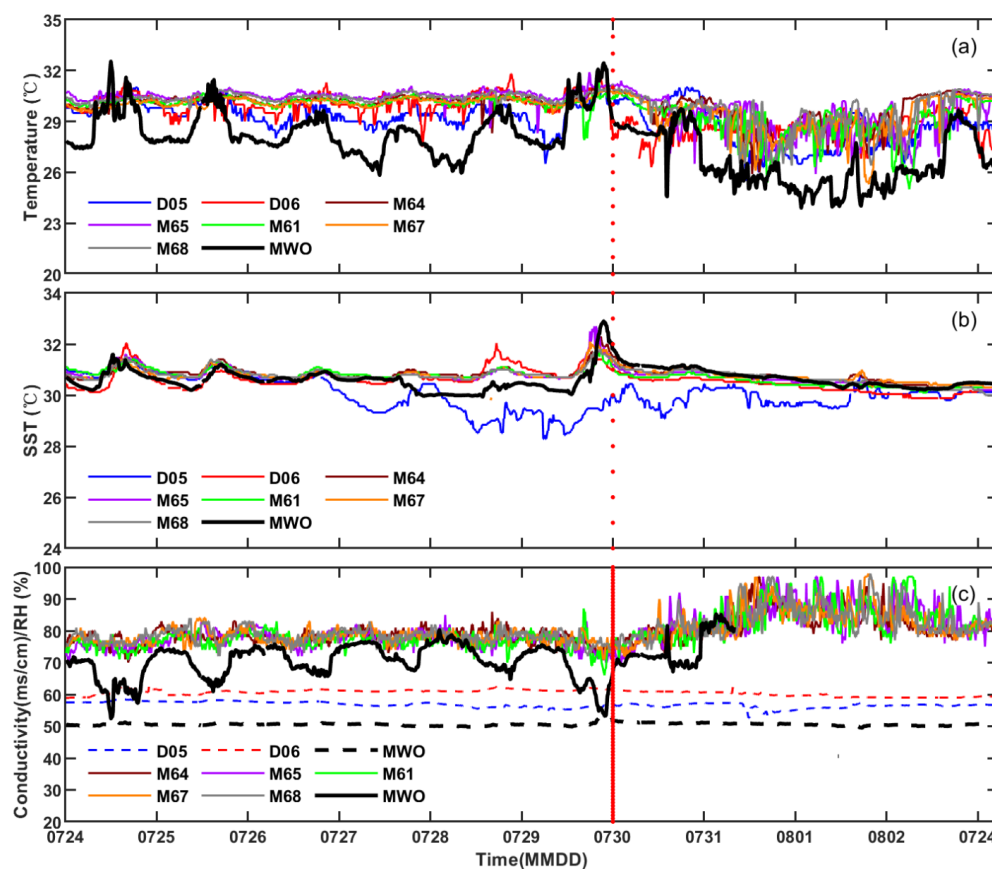
245 In addition, seawater conductivity and relative humidity (RH) can be obtained
246 from MWO. However, only the two drifting buoys can provide seawater conductivity
247 measurement, and the mooring buoys can provide relative humidity (RH)
248 measurement. Hence, the seawater conductivity and RH measured from MWO are
249 compared with those from the corresponding available buoys and displayed in Fig.5c.

250 Firstly, the seawater conductivity measured on MWO and two drifting buoys are
251 very different, but the detailed values of each instrument are constant throughout the
252 entire period. The conductivity measurement from D06 buoy is the highest, generally
253 exceeding 60 mscm⁻¹, followed by D05 buoy, which is basically around 57 mscm⁻¹,
254 and the lowest is about 50 mscm⁻¹ from MWO.

255 The RH difference between mooring buoys and MWO shown in Fig.5c is only



256 available in the first stage because the humidity sensor on MWO stopped working
257 after July 30. The RH variations are similar to those of air temperature, that is, RH
258 from MWO is mostly lower than that from mooring buoy, especially in the daytime.
259 The diurnal variations of RH measured from MWO are more significant while RH
260 differences among the mooring buoys are smaller and stable in the first stage.



261
262 **Fig.5.** Same as Fig.3, except for (a) air temperature, (b) SST, and (c) seawater conductivity (dotted
263 line) for drifting buoys and RH (solid line) for the mooring buoys.

264

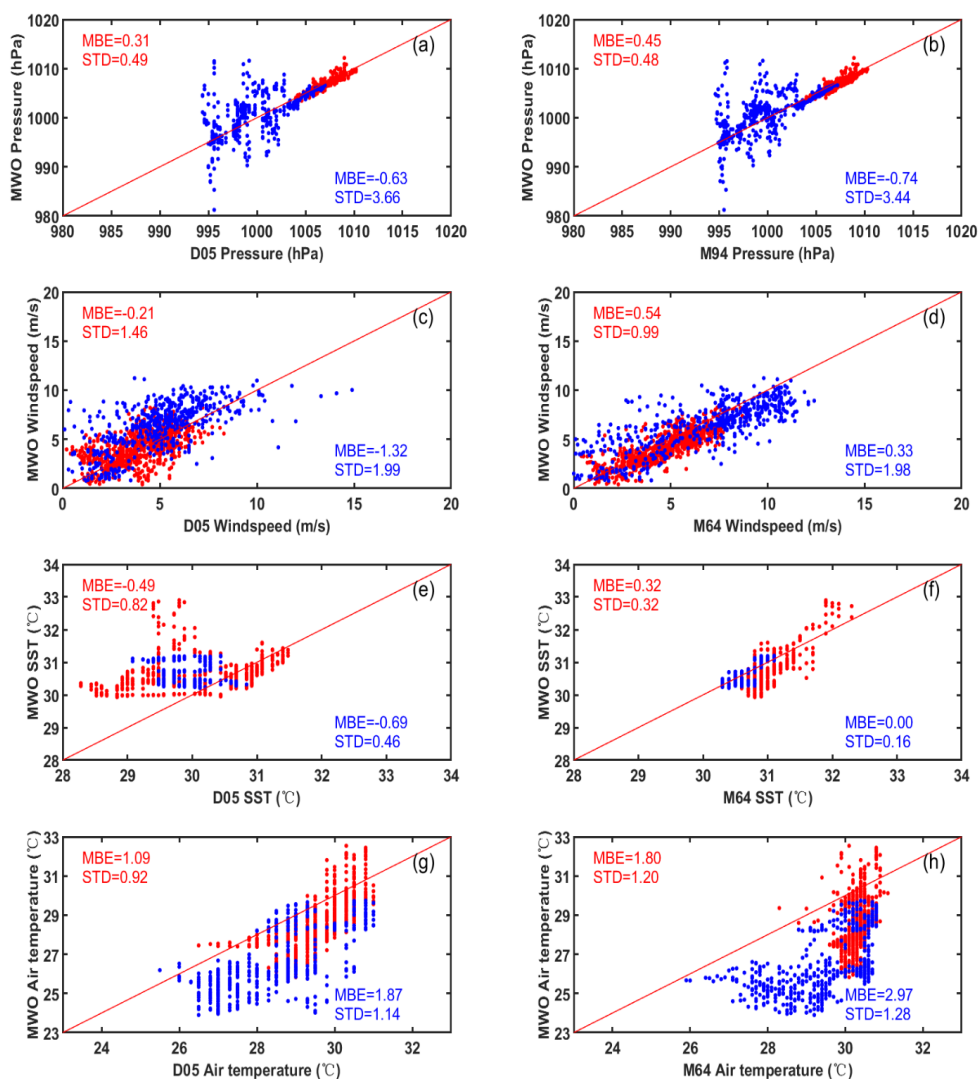
265 To better see the influence of typhoon moving on MWO observations, Fig.6
266 shows the scattering plots of meteorological variables observed by MWO and the



267 nearest buoys, including the drifting D05 and the mooring M94. The color samples
268 and their corresponding statistical results are used to quantify the observations
269 differences before (in red) and after the arrival of typhoons (in blue). Firstly, before the
270 arrival of the typhoon, air pressure differences between MWO and both buoys are in
271 good agreement, as shown in the red samples in Fig.6a,b. Both air pressure differences
272 are very close and smaller, such as mean bias error (MBE) and standard deviation
273 (STD) less than 0.5 hPa. However, in the second stage, the pressure difference is
274 significantly enhanced when MWO approaches the center of the typhoon, shown as
275 the highly scattered blue samples in Fig. 6a, b, with corresponding STD up to 3.5 hPa.

276 The wind speed measurements from both buoys and MWO have good
277 consistency in both stages, which is reflected in the good overlap of the red and blue
278 samples in Fig.6c,d, and the corresponding MBE and STD are very close. For SST
279 shown in Fig.6e,f, it is seen that the observations between MWO and the mooring
280 M64 buoy are quite consistent with a difference of less than 0.3°C before and after the
281 coming of the typhoon. The SST measurements from the drifting buoy D05 are more
282 scattering with those from MWO the most of time, especially significantly decreased
283 by about $1\text{-}2^{\circ}\text{C}$ from July 27 to Aug. 1st as shown in Fig.5b. The overall MBE and
284 STD of SST difference are less than 1.0°C due to partial overlap of the samples.

285



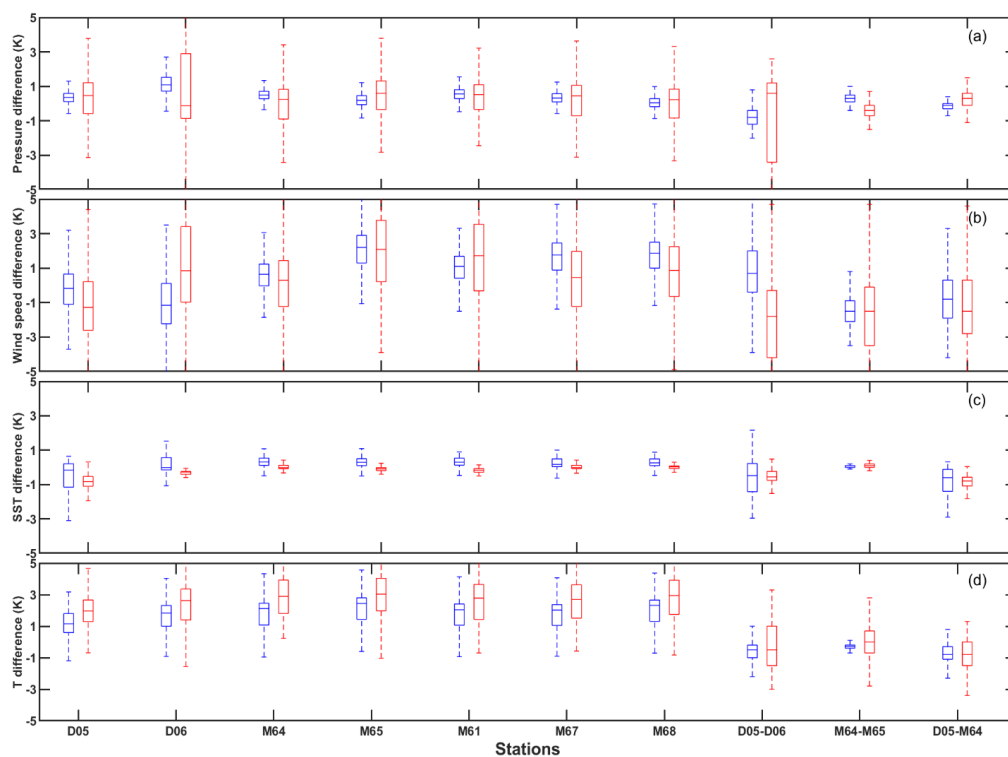
286

287 Fig.6 Scattering plots of observations from the nearest buoys and MWO, with the drifted D05 in
288 the left column and the mooring M64 in the right column. From top to bottom, they are air pressure,
289 wind speed, SST, and air temperature, respectively.

290 Regarding air temperature, the observations from MWO show significant
291 fluctuations, while the mooring M64 shown in Fig.6h mostly fixes around 30°C in the
292 first stage. In the second stage, the air temperature measured from MWO is lower than



293 that measured from both buoys, for example, the MBE corresponding to buoys D05
294 and M64 is close to 1.9°C and 3°C , respectively. Relatively, the changed trends of air
295 temperature measured from MWO and D05 have good consistency in both stages.



296
297 Fig. 7. The boxplots of observations difference (blue: the first stage; red: the second stage) between
298 MWO and seven buoys, as well as between buoys (i.e. D05 and D06, M64 and M65, and D05 and
299 M64). The observations from up to bottom are air pressure (a), wind speed (b), SST (c), and air
300 temperature (d).

301

302 To better understand the observed differences between MWO and buoys, as well
303 as between buoys, the boxplots in Fig. 7 show the distribution of their differences in
304 pressure, wind speed, SST, and air temperature during the first (blue) and second (red)
305 stages. The center marker in each box indicates the median, and the bottom and top
306 edges of the box indicate the 25th and 75th percentiles, respectively. The first seven



307 buoys reflect the difference between the buoy observations and MWO observations.
308 The last three reflect differences in observations between buoys, including the two
309 drifting buoys D05 and D06, the nearest (M64) and farthest mooring buoys(M65)
310 from the MWO, and the nearest drifting D05 and moored M64 from the MWO.

311 The pressure difference in Fig. 7a shows a clear change in the first and second
312 stage. Before the arrival of the typhoon, the pressure difference between MWO and
313 the buoys are close to zero, and the magnitude of the differences between MWO and
314 the buoys vary relatively uniformly, indicating that the pressure measured by MWO
315 has the same level of accuracy as those measured by buoys under normal sea
316 conditions. In the second stage, the range of pressure difference between MWO and
317 buoy is 2-3 times larger than that in the first stage, but the median value of pressure
318 difference is still relatively close, mostly within 1hPa. Relatively, the pressure
319 differences between the buoys in both stages are relatively small and stable, except for
320 the farthest D06.

321 The median difference of wind speed between MWO and the buoys are mostly
322 within 1 m/s as shown in Fig. 7b. The wind speed difference in the second stage is
323 significantly larger than that in the first stage. The wind speed difference between
324 buoys seems to increase with the distance between buoys, as in the more distant buoys
325 D06 and M65. In general, the wind speed differences between MWO and buoys are
326 comparable to the wind speed differences between buoys.

327 For the SST in Fig. 7c, the observed differences between MWO and the moored
328 buoys are very small throughout the period and even better in the second stage. In



329 contrast, the difference in SST between MWO and the two drifting buoys is not as
330 good as that between the moored buoys, especially for the closest buoy, D05, which
331 fluctuates more in the first period, which may indicate that the SST quality of D05
332 buoy is not as good as its other measurements, such as pressure and wind speed.

333 The difference in air temperature between MWO and the buoys (Fig. 7d) is more
334 pronounced than the difference in SST. Because of the lower temperature measured by
335 MWO, the median of temperature difference with the buoys is mostly positive, e.g., 1
336 K in the first stage and 2 K in the second stage, while the temperature difference
337 between the buoys is smaller in the first stage and increases significantly by a factor of
338 2-3 in the second stage.

339 **4 Discussions**

340 In this paper, we first used 1-minute MWO in-situ observation data to monitor the
341 changes in air pressure, wind field, temperature, and humidity before and after the
342 arrival of typhoons. In particular, the air pressure significantly decreased from 1010
343 hPa under normal sea conditions to 980 hPa at the time when MWO crossed the center
344 of the typhoon. During this period the air pressure underwent obvious and detailed
345 fluctuations, which cannot be provided by previous observations. In addition, the wind
346 field reflected the detailed and obvious fluctuations when the typhoon approached.
347 The air temperature and relative humidity in the lower layers of the sea exhibited
348 obvious diurnal variations. In contrast, SST is more stable, showing slight changes
349 before and after the typhoon.

350 Further comparison with buoys observations during the same period revealed that



351 under normal sea conditions before the arrival of the typhoon, the air pressure and
352 wind speed measured by MWO and buoys showed good consistency, especially the
353 difference in air pressure was only less than 0.5hPa, and the wind speed difference was
354 less than 0.5 m/s. Moreover, the difference between MWO and buoys was comparable
355 to that of multiple buoys, indicating that the measurement accuracy of air pressure and
356 wind speed on MWO was equivalent to that of the buoys under normal sea conditions.
357 With the arrival of the typhoon, the air pressure measured on MWO fluctuated greatly,
358 while the corresponding measurements on the buoys were more stable, resulting in a
359 significant pressure difference between MWO and the buoys. This may mainly be
360 related to the location where MWO crossed the center of the typhoon. In addition, as
361 the typhoon departed, the air pressure and temperature measured on MWO showed
362 abnormally high values around 14:00 on August 2nd, and then returned to normal
363 range at night, which may be related to unknown external interference.

364 The trend of wind speed change between MWO and the buoys was more
365 consistent before and after the arrival of the typhoon. When MWO was closest to the
366 center of the typhoon, the wind speed change between MWO and the buoys was
367 slightly misaligned.

368 For the air temperature and relative humidity under normal sea conditions,
369 measurements made by the mooring buoys were relatively constant and little
370 variations in a day; the corresponding drifting buoys measurements showed slight
371 diurnal fluctuations; MWO measurements fluctuated significantly from day to night.
372 This may be related to the mounting height of the sensor. Usually, the sensor on the



373 mooring buoy can reach up to 10m, on the drifting buoy it may be about 1.5m, and on
374 MWO it is close to 1.2m. The closer the sensor is to the water's surface, the more
375 obvious the impact on the marine environment.

376 Compared with other variables, the SST variation before and after the typhoon's
377 arrival was weak and appeared relatively stable. In particular, the SST measurements
378 from MWO and the mooring buoys were very close throughout the period, and even
379 better in the second stage. However, the larger difference in SST between MWO and
380 the nearest drifting buoy may be caused by the quality of the SST measurement from
381 the latter.

382 **5 Summary**

383 During the typhoon observation experiment in the South China Sea in
384 July-August 2020, MWO completed long-term continuous observations, especially by
385 actively approaching the center of Typhoon Sinlaku in the deep sea. The in-situ
386 meteorological and hydrological observations obtained by MWO were evaluated by
387 comparing them with the observations made by two types of buoys during the
388 evolution of Typhoon Sinlaku. We obtained some preliminary results as follows.

389 1) Before the arrival of the typhoon, air pressure and wind speed measured by
390 MWO and the buoys were in good agreement, with the difference in air pressure less
391 than 0.5hPa and the difference in wind speed less than 0.5 m/s, indicating that the
392 measurement accuracy of air pressure and wind speed obtained by the two methods is
393 comparable under normal sea conditions.

394 2) The SST observations of MWO and the mooring buoys show highly consistent



395 in the entire period, and even a smaller difference in SST after the arrival of the
396 typhoon, demonstrating the high stability and accuracy of SST measurements from
397 MWO during the typhoon evolution.

398 3) The air temperature and relative humidity measured from MWO have obvious
399 diurnal variations and are generally lower than those from the buoys, which may be
400 related to the mounting height of the sensor.

401 4) When actively approaching the typhoon center, the air pressure measured by
402 MWO can reflect some drastic and subtle changes, such as a sudden drop to 980 hPa,
403 which is difficult to obtain by other observation methods.

404 As a mobile meteorological and oceanographic observation station, MWO has
405 shown its unique advantages over traditional observation methods. Although we only
406 analyzed and evaluated the in-situ observations obtained in one individual case of
407 MWO crossing the Typhoon Sinlaku in this paper, the results preliminary demonstrate
408 the reliable observation capability of MWO. For better monitoring of typhoon systems,
409 it will be necessary to deploy a meteorological and hydrological observation network
410 composed of multiple MWOs in the future, which will provide comprehensive in-situ
411 observations on spatial and temporal scales required for forecasting, warnings, and
412 research of marine meteorological hazards.

413 **Acknowledgments.** This work is supported by the National Natural Science
414 Foundation of China (Grant No. 41627808), the Key Technologies Research and
415 Development Program (Grant No. 2018YFC1506401), the Shanghai Typhon Reseach
416 Foundation (Grant No. TFJJ202101). We wish to express our sincere gratitude to



417 Beijing Chunyi Aviation Technology Co., Ltd., Hainan Meteorological Service, Wang
418 Hu, and Wang Chunhua of Qionghai Meteorological Service, and all personnel who
419 participated in this experiment.

420 REFERENCES

- 421 Bell, M. M., Montgomery M. T., and Emanuel K. A.: Air-sea enthalpy and momentum exchange at
422 major hurricane wind speeds observed during CBLAST, *Journal of Atmospheric Sciences*, 69,
423 3197–3222, 2012.
- 424 Bender, M. A., Ginis I., Tuleya R., Thomas B., and Marchok T.: The operational GFDL coupled
425 hurricane-ocean prediction system and a summary of its performance, *Monthly Weather Review*,
426 135(12), 3965–3989, 2007.
- 427 Black, P. G., and Coauthors: Air-sea exchange in hurricanes: Synthesis of observations from the
428 coupled boundary layer air-sea transfer experiment, *Bulletin of the American Meteorological
429 Society*, 88(3), 357–374, 2007.
- 430 Chen, H. B., Li J., Ma S. Q., Hu S. Z.: Progress of the marine meteorological observation
431 technologies, *China Association for Science and Technology*, 37, 91-97, 2019.
- 432 Chen. H. B., LI J., He W., Ma S., Wei Y., Pan J., Zhao Y., Zhang X., Hu S.: IAP's solar-powered
433 unmanned surface vehicle actively passes through the center of Typhoon Sinlaku (2020), *Adv.
434 Atmos. Sci.*, 38(4), 538–545, 2021.
- 435 Dai, H. L., Mou N. X., Wang C. Y., and Tian M. Y.: Development status and trend of ocean buoy in
436 China, *Meteorological, Hydrological and Marine Instruments*, 118–121, 125, 2014.
- 437 Emanuel, K., and Center L.: 100 Years of Progress in Tropical Cyclone Research, *Meteorological
438 Monographs*, 59, 15.1-15.68, 2018
- 439 Ito, K. and Wu C. C.: Typhoon-position-oriented sensitivity analysis. Part I: Theory and verification,
440 *Journal of Atmospheric Sciences*, 70, 2525-2546, 2013.
- 441 Lei, X. T.: Overview of the development of Typhoon scientific research in China in the past century,
442 *Science China: Earth Sciences*, 50(3), 321-338, 2020.
- 443 Lenan, L. and Melville W.K.: Autonomous surface vehicle measurements of the ocean's response to
444 tropical cyclone Freda, *Journal of Atmospheric and Oceanic Technology*, 31(10), 2169–2190,
445 2014.
- 446 Lorsolo, S., Schroeder J. L., Dodge P., and Marks F.: An observational study of hurricane boundary
447 layer small-scale coherent structures, *Mon. Wea. Rev.*, 136, 2871–2893, 2008.
- 448 Morrison, I., Businger S., Marks F., Dodge P., and Businger J. A.: An observational case for the
449 prevalence of roll vortices in the hurricane boundary layer, *J. Atmos. Sci.*, 62, 2662–2673, 2005.
- 450 Qin G., Lei Y., Li X., Cao X., Wang Y., Xu M., Zhou W.: Operational assessment of domestic marine
451 meteorological drifting buoys, *Meteorological Science and Technology*, 50(4), 467-475, 2022.
- 452 Rogers, R., S. Abernethy, A. Aksoy, et al.: NOAA's hurricane intensity forecasting experiment: A
453 progress report, *Bulletin of the American Meteorological Society*, 94, 859-882, 2013.
- 454 Sanford, T. B., Price J. F., Girton J. B., and Webb D. C.: Highly resolved observations and
455 simulations of the ocean response to a hurricane, *Geophysical Research Letters*, 34 (13),
456 L13604, 2007.



- 457 Schmidt K.M., Swart S., Reason C., Nicholson S.A.: Evaluation of satellite and reanalysis wind
458 products with in situ wave glider wind observations in the Southern Ocean, *J Atmos Ocean*
459 *Technol*, 34:2551–2568, 2017.
- 460 Thomson, J., and Girton J.: Sustained measurements of Southern Ocean air-sea coupling from a
461 Wave Glider autonomous surface vehicle. *Oceanography* 30(2):104–109,2017.
- 462 Wynn, R. B., and Coauthors: Autonomous Underwater Vehicles (AUVs): Their past, present and
463 future contributions to the advancement of marine geoscience, *Marine Geology*, 352, 451–468,
464 2014.
- 465 Xu, X. F, Gu J. F., Li Y. P.: Marine meteorological disaster [M]. Beijing: China Meteorological Press,
466 1-4,2009.
- 467 Yang, L., Wang D.X., Huang J. et al.: Toward a mesoscale hydrological and marine meteorological
468 observation network in the South China Sea, *Bulletin of the American Meteorological Society*,
469 96(7), 1117–1135, 2015.
- 470 Yu, M. G.: An introduction to military oceanography [M]. Beijing: The People's Liberation Army
471 Press, 65-67, 2003.
- 472 Zhang X , Li L.X., Yang R., et al.:Comprehensive Marine Observing Experiment Based on
473 High-Altitude Large Unmanned Aerial Vehicle(South China Sea Experiment2020 of the "Petrel
474 Project"), *Advances in Atmospheric Sciences*, **38**(4), 528–535, 2021.
- 475 Zheng, G. G, Chen H. B., Bian J. C., et al.: Atmospheric sciences entering the 21st century [M].
476 Beijing: China Meteorological Press, 21-25, 2008.
- 477 Wu L.G., Liu Q.Y., Zhou X. Y.:A review on fine-scale structures in tropical cyclone boundary layer,
478 *Journal of the Meteorological Sciences*, 40(1),1-10, 2020.
- 479 Wurman J, Kosiba K.:The role of small-scale vortices in enhancing surface winds and damage in
480 Hurricane Harvey (2017), *Mon. Wea. Rev.*, 146, 713-722,2018.
- 481